Electronic Supplementary Information (ESI)

Fluctuation Correlations as Major Determinants of Structure- and Dynamics-Driven Allosteric Effects

Miao Yu,[a] Yixin Chen,[a] Zi-Le Wang[b] and Zhirong Liu[ac*]

[a.] College of Chemistry and Molecular Engineering, Peking University, Beijing 100871, China. Email: LiuZhiRong@pku.edu.cn

[b.] Department of Physics, Tsinghua University, Beijing 100084, China

[c.] Center for Quantitative Biology, State Key Laboratory for Structural Chemistry of Unstable and Stable Species, and BNLMS, Peking University, Beijing 100871, China

Text S1 A simplified four-bead model with analytical solution

Here we consider a simplified four-bead model where analytical solutions are available. The system is one-dimensional, and a periodic boundary condition (or a ring configuration) is assumed. To enable an analytical solution, we further assume a two-fold symmetry as demonstrated in the schematic below, i.e., $k_{12} = k_{34} \equiv k_1$.

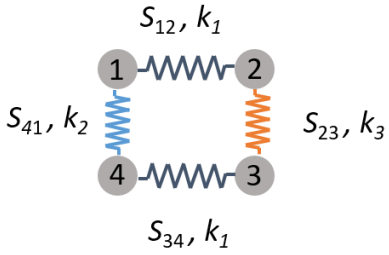

Schematic of the simplified four-bead system with two-fold symmetry. The force constant and the equilibrium length of springs are denoted by k and S, respectively.

S1.1 Diagonalization of the Hessian matrix (eigenvalues and eigenvectors)

The Hessian matrix of the system:

$$\boldsymbol{H} = \begin{bmatrix} k_1 + k_2 & -k_1 & 0 & -k_2 \\ -k_1 & k_1 + k_3 & -k_3 & 0 \\ 0 & -k_3 & k_1 + k_3 & -k_1 \\ -k_2 & 0 & -k_1 & k_1 + k_2 \end{bmatrix}. \tag{S1}$$

The eigenvalues $\{\lambda_n\}$ and eigenvectors $\{\boldsymbol{u}^{(n)}\}$ of the system are to be solved from the eigen equation:

$$\begin{bmatrix} (k_1+k_2)-\lambda & -k_1 & 0 & -k_2 \\ -k_1 & (k_1+k_3)-\lambda & -k_3 & 0 \\ 0 & -k_3 & (k_1+k_3)-\lambda & -k_1 \\ -k_2 & 0 & -k_1 & (k_1+k_2)-\lambda \end{bmatrix} \begin{bmatrix} u_1 \\ u_2 \\ u_3 \\ u_4 \end{bmatrix} = 0.$$

(S2)

Considering the two-fold symmetry of the system, the solutions have a definite parity. With an even parity, i.e.,

$$\begin{cases} u_4 = u_1 \\ u_3 = u_2 \end{cases},$$

(S3)

only one non-zero solution is found (while a trivial translational solution is $\lambda = 0$):

$$\lambda_1 = 2k_1.$$

(S4)

The corresponding eigenvector is

$$\boldsymbol{u}^{(1)} \equiv \begin{bmatrix} u_1 \\ u_2 \\ u_3 \\ u_4 \end{bmatrix} = \frac{1}{2} \begin{bmatrix} 1 \\ -1 \\ -1 \\ 1 \end{bmatrix}.$$

(S5)

With an odd parity, i.e.,

$$\begin{cases} u_4 = -u_1 \\ u_3 = -u_2 \end{cases},$$

(S6)

two non-zero solutions are derived:

$$\lambda_{2,3} = \lambda_{\pm} = k_1 + k_2 + k_3 \pm \sqrt{(k_1+k_2+k_3)^2 - (2k_1k_2 + 2k_1k_3 + 4k_2k_2)}$$

$$= k_1 + k_2 + k_3 \pm \sqrt{k_1^2 + (k_2 - k_3)^2}.$$

(S7)

The corresponding eigenvectors are

$$\boldsymbol{u}^{(2,3)} \equiv \begin{bmatrix} u_1 \\ u_2 \\ u_3 \\ u_4 \end{bmatrix}$$

$$= \frac{1}{2\sqrt{k_1^2 + (k_2-k_3)^2 \pm (k_2-k_3)\sqrt{k_1^2 + (k_2-k_3)^2}}} \begin{bmatrix} -k_1 \\ k_3 - k_2 \pm \sqrt{k_1^2 + (k_2-k_3)^2} \\ -u_2 \\ -u_1 \end{bmatrix}$$

(S8)

S1.2 Covariance of equilibrium fluctuations

With the equation for the covariance of equilibrium fluctuations,

$$\langle \Delta \boldsymbol{r}_i \Delta \boldsymbol{r}_j \rangle = k_{\mathrm{B}} T \sum_n \frac{u_i^{(n)} u_j^{(n)}}{\lambda_n},$$

(S9)

and Eqs. (S4, S5, S7, S8) above, it yields:

$$\frac{\langle \Delta d_{23} \Delta d_{41} \rangle}{k_{\mathrm{B}} T} \equiv \frac{\langle (\Delta \boldsymbol{r}_3 - \Delta \boldsymbol{r}_2) \cdot (\Delta \boldsymbol{r}_1 - \Delta \boldsymbol{r}_4) \rangle}{k_{\mathrm{B}} T} = -\frac{k_1}{k_1 k_2 + k_1 k_3 + 2 k_2 k_3},$$

(S10)

S1.3 Dynamics-driven allosteric effect (perturbation on force constant)

The free energy can be written as a function of all the non-zero eigenvalues:

$$F = C_0 + \frac{k_B T}{2} \ln \prod_{n=1,2,3} \lambda_n,$$

(S11)

where C_0 is a constant irrelevant to λ_n. For arbitrary dynamics mutations on the springs 2-3 and 4-1, i.e.,

$$\begin{cases} k_3 \to k_3 + \Delta k_{23} \\ k_2 \to k_2 + \Delta k_{41} \end{cases},$$

(S12)

a combination of Eqs. (S4, S7, S11, S12) gives

$$\begin{aligned} &F^{\mathrm{mut}(2-3,4-1)}(\Delta k_{23}, \Delta k_{41}) \\ &= C_0 + \frac{k_B T}{2} \ln(2k_1) + \frac{k_B T}{2} \ln\{(k_1 + k_2 + k_3 + \Delta k_{23} + \Delta k_{41})^2 - [k_1^2 + (k_2 - k_3 + \Delta k_{23} - \Delta k_{41})^2]\}. \end{aligned}$$

(S13)

Therefore, the allosteric coupling free energy is

$$\begin{aligned} \Delta\Delta F &= F^{\mathrm{mut}(2-3,4-1)}(\Delta k_{23}, \Delta k_{41}) - F^{\mathrm{mut}(2-3,4-1)}(\Delta k_{23}, 0) - F^{\mathrm{mut}(2-3,4-1)}(0, \Delta k_{41}) + F^{\mathrm{mut}(2-3,4-1)}(0,0) \\ &\cong \left. \frac{\partial^2 F^{\mathrm{mut}(2-3,4-1)}(\Delta k_{23}, \Delta k_{41})}{\partial \Delta k_{23} \partial \Delta k_{41}} \right|_0 \Delta k_{23} \Delta k_{41} \\ &= -\frac{k_{\mathrm{B}} T}{2} \frac{k_1^2}{(k_1 k_2 + k_1 k_3 + 2 k_2 k_3)^2} \Delta k_{23} \Delta k_{41} \end{aligned}$$

(S14)

up to the second-order expansion. Comparing Eq. (S10) and Eq. (S14), we finally obtain the dynamics-driven allosteric effect:

$$\Delta\Delta F = -\frac{1}{2 k_{\mathrm{B}} T} \langle \Delta d_{23} \Delta d_{41} \rangle^2 \Delta k_{23} \Delta k_{41},$$

(S15)

which is in fully agreement with Eq. (26) of the main text.

S1.4 Structure-driven allosteric effect (perturbation on bead radius)

Consider perturbation Δa_{23}, Δa_{41} on the equilibrium length of springs 2-3 and 4-1, the potential energy of the system becomes

$$V = \frac{k_1}{2} \left({\Delta x_{12}}^2 + {\Delta x_{34}}^2 \right) + \frac{k_3}{2} (\Delta x_{23} - \Delta a_{23})^2 + \frac{k_2}{2} (\Delta x_{41} - \Delta a_{41})^2.$$

(S16)

The period-boundary condition requires that

$$\Delta x_{12} + \Delta x_{23} + \Delta x_{34} + \Delta x_{41} = 0. \tag{S17}$$

Together with the two-fold symmetry of the system, we thus have

$$\Delta x_{12} = \Delta x_{34} = -\frac{\Delta x_{23} + \Delta x_{41}}{2} \tag{S18}$$

for the energy minimum state, so

$$V = \frac{k_1}{4}(\Delta x_{23} + \Delta x_{41})^2 + \frac{k_3}{2}(\Delta x_{23} - \Delta a_{23})^2 + \frac{k_2}{2}(\Delta x_{41} - \Delta a_{41})^2. \tag{S19}$$

The solution for the energy minimum state is

$$\begin{cases} \Delta x_{23} = \dfrac{2k_3(k_1 + 2k_2)\Delta a_{23} - 2k_2 k_1 \Delta a_{41}}{(k_1 + 2k_3)(k_1 + k_2) - k_1^2} \\ \Delta x_{41} = \dfrac{2k_2(k_1 + 2k_3)\Delta a_{41} - 2k_3 k_1 \Delta a_{23}}{(k_1 + 2k_3)(k_1 + 2k_2) - k_1^2} \end{cases}. \tag{S20}$$

and

$$V_0(\Delta a_{23}, \Delta a_{41}) = \frac{k_1 k_2 k_3}{2(k_1 k_2 + k_1 k_3 + 2k_2 k_3)}(\Delta a_{23} + \Delta a_{41})^2.$$

So the allosteric effect is

$$\begin{aligned} \Delta\Delta V_0 &= V_0(\Delta a_{23}, \Delta a_{41}) - V_0(\Delta a_{23}, 0) - V_0(0, \Delta a_{41}) + V_0(0,0) \\ &= \frac{k_1 k_2 k_3}{k_1 k_2 + k_1 k_3 + 2k_2 k_3}\Delta a_{23}\Delta a_{41}. \end{aligned} \tag{S21}$$

Considering Eq. (S10), we finally get

$$\Delta\Delta V_0 = -\frac{k_2 k_3}{k_B T}\langle \Delta d_{23}\Delta d_{41}\rangle \Delta a_{23}\Delta a_{41}. \tag{S22}$$

It is consistent with Eq. (39) in the main text.

Table S1. A summary on the Pearson's R values between various quantities.

y	x	R values	source
Dynamics-driven allostery			
ΔF (a single spring perturbed)	$C_{ij}^{(\mathrm{DP})}$	0.12	Fig. 4(a)
	$\langle\lvert\Delta\mathbf{r}_i\rvert^2\rangle^{1/2}\,\langle\lvert\Delta\mathbf{r}_j\rvert^2\rangle^{1/2}$	0.42	Fig. 4(b)
	$\langle(\Delta d_{ij})^2\rangle$	1.000	Fig. 4(c)
$\Delta F_{\mathrm{mut\_}i}$	n_i	0.88	Fig. 5(a)
$\Delta F_{\mathrm{mut\_}i}/n_i$	$\langle\lvert\Delta\mathbf{r}_i\rvert^2\rangle^{1/2}$	0.68	Fig. 5(b) inset
$\Delta F_{\mathrm{mut\_}i}$	$\langle(\Delta d_{i*})^2\rangle$	1.000	Fig. 5(c)
		0.997	Fig. 5(d)
$\Delta\Delta F$	$\langle\Delta d_{i*}\Delta d_{k*}\rangle^2$	-1.000	Fig. 6(b)
		-1.000, -0.998, -0.994, -0.994	Fig. 6(d)
	$C_{ik}^{(\mathrm{DP})}$	-0.50	Fig. 6(c)
Structure-driven allostery			
$\Delta V_{0,\mathrm{mut\_}i}$	n_i	0.86	Fig. 7(a)
$\Delta V_{0,\mathrm{mut\_}i} - n_i\gamma(\Delta a)^2/2$	$\langle\Delta d_{i*}\Delta d_{i*}\rangle$	0.999	Fig. 7(c)
$\lvert\Delta\Delta V_0\rvert$	$C_{ik}^{(\mathrm{DP})}$	0.57	Fig. 8(b)
	$\langle\Delta\mathbf{r}_i\cdot\Delta\mathbf{r}_k\rangle$	0.38	Fig. 8(c)
$\Delta\Delta V_0$	$C_{ik}^{(\mathrm{DP})}$	0.19	Fig. 8(b)
	$\langle\Delta\mathbf{r}_i\cdot\Delta\mathbf{r}_k\rangle$	0.11	Fig. 8(c)
	$\langle\Delta d_{i*}\Delta d_{k*}\rangle$	-1.00	Fig. 8(d)
		-1.00, -0.97, -0.85, -0.98	Fig. 8(e)

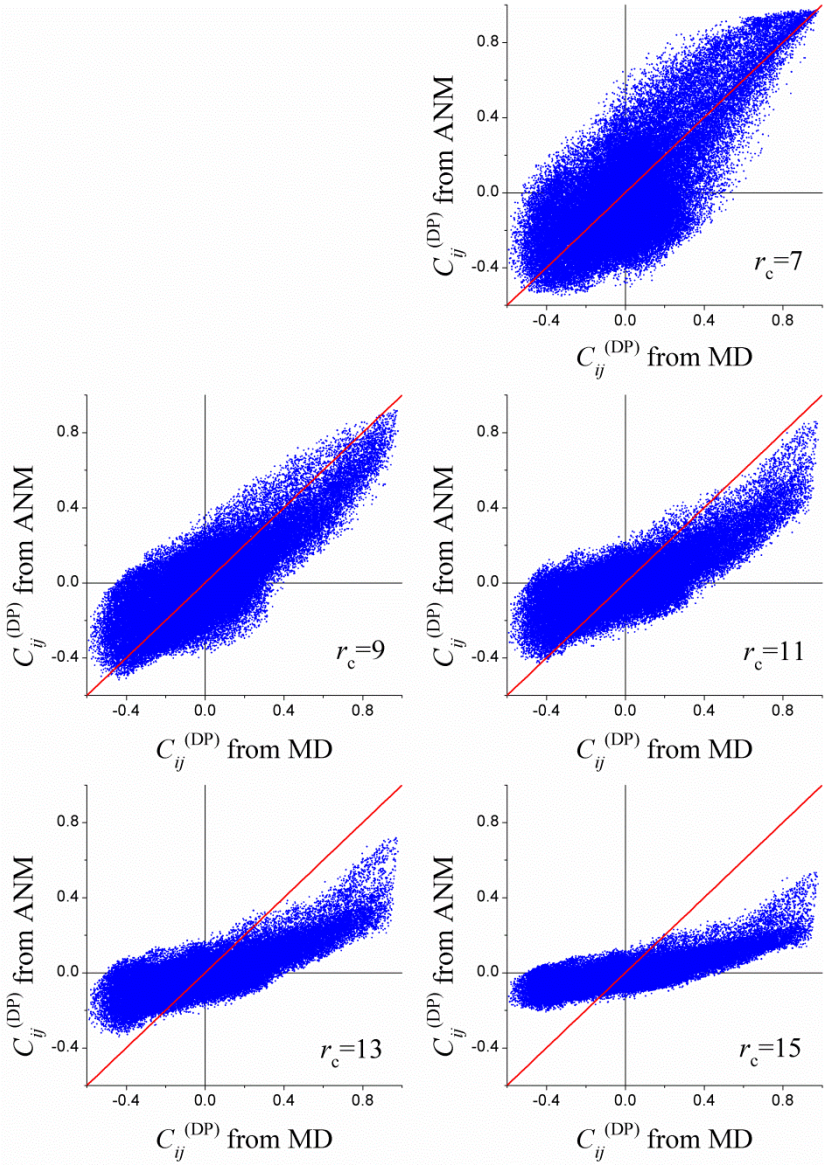

FIGURE S1 The correlation between $C_{ij}^{(\mathrm{DP})}$ of Gō-like model (MD) and ANM for the protein CAP with different cutoff distance r_c (in Å). Solid lines indicate the ideal curve of $y = x$.

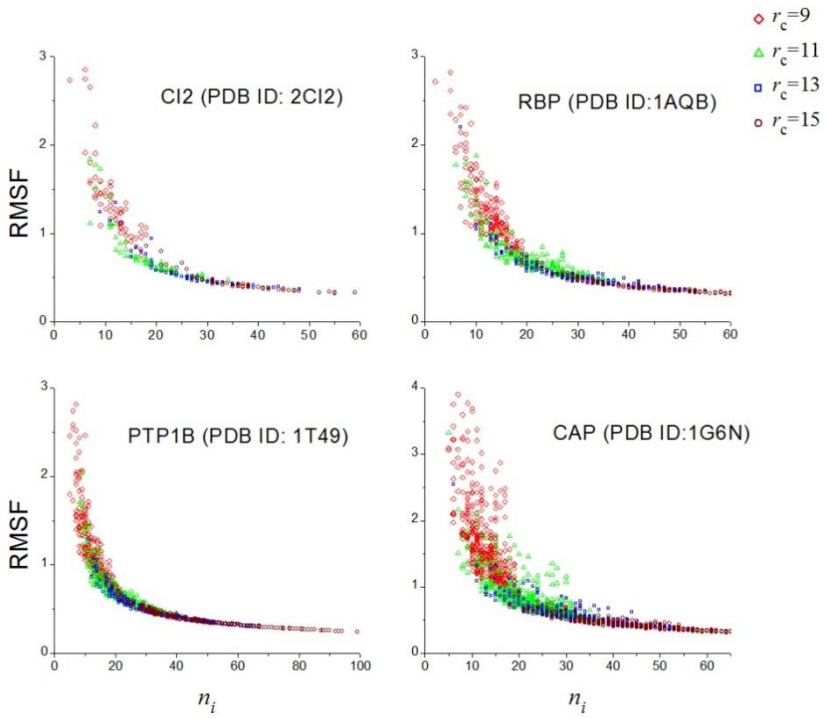

FIGURE S2 Root-mean-square-fluctuation (RMSF), i.e., $\langle|\Delta\mathbf{r}_i|^2\rangle^{1/2}$, as a function of the number of springs connected to the residue (n_i), calculated from ANM with parameters $m = 0.11$ kg/mol, $\gamma = 1.0$ kcal/(mol·Å^2) and various r_c values as indicated in the graphs. Four systems were examined: chymotrypsin inhibitor 2 (CI2), pig plasma retinol binding protein (RBP), tyrosine-protein phosphatase nonreceptor type 1 (PTP1B) and the catabolite activator protein (CAP).

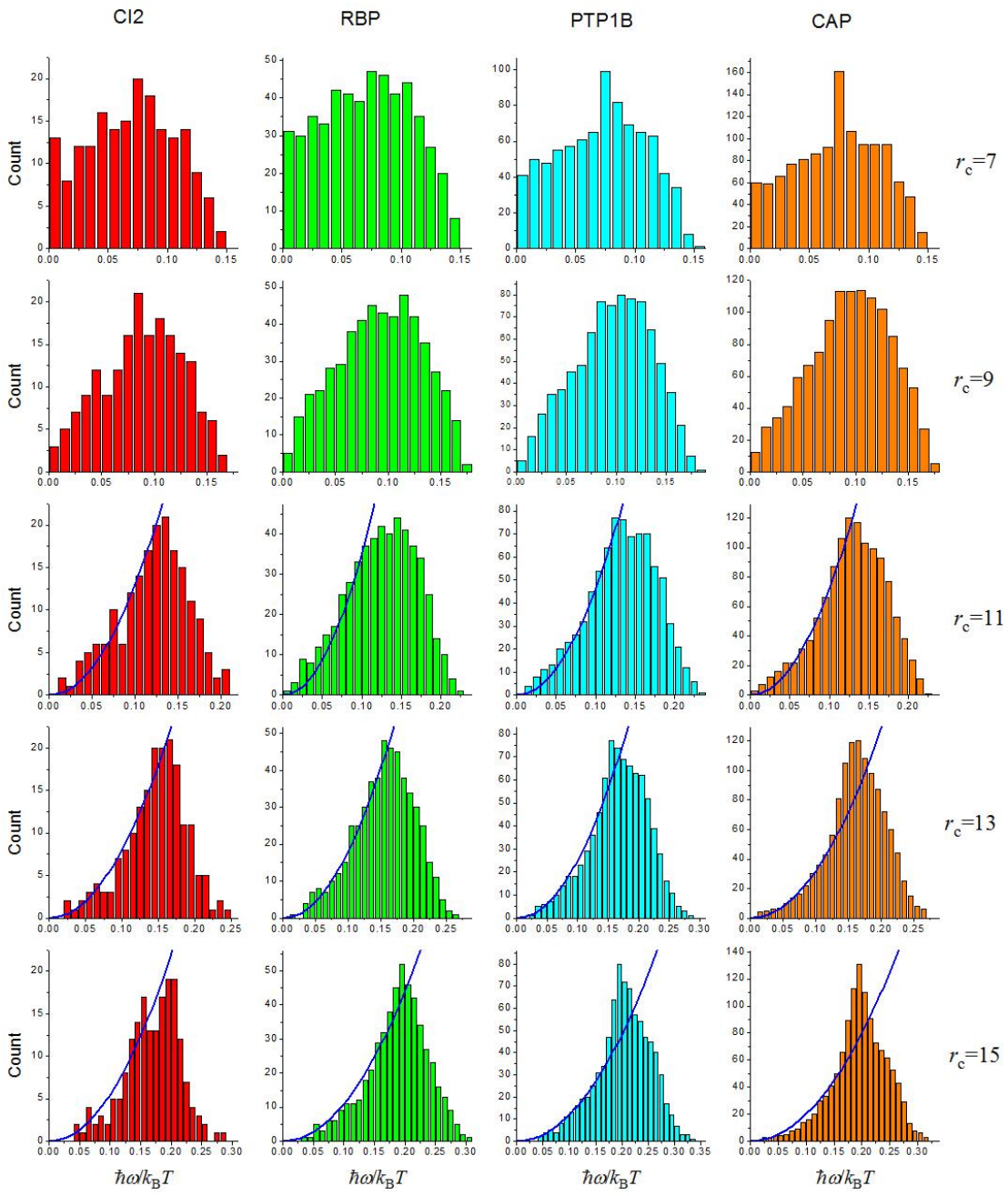

FIGURE S3 Distribution of vibration frequencies for four protein systems (from left to right) calculated from ANM with various r_c values (from top to bottom). $m = 0.11$ kg/mol, $\gamma = 1.0$ kcal/(mol·Å^2). Solid lines indicate the prediction given by the Debye model of solids, i.e., $P(\omega) \propto \omega^2$, which can be used to well describe the distribution of lower frequencies. In addition, the frequencies satisfy $\hbar\omega < k_BT$, so the high temperature approximation is satisfied and the Boltzmann statistics can be applied reliably.

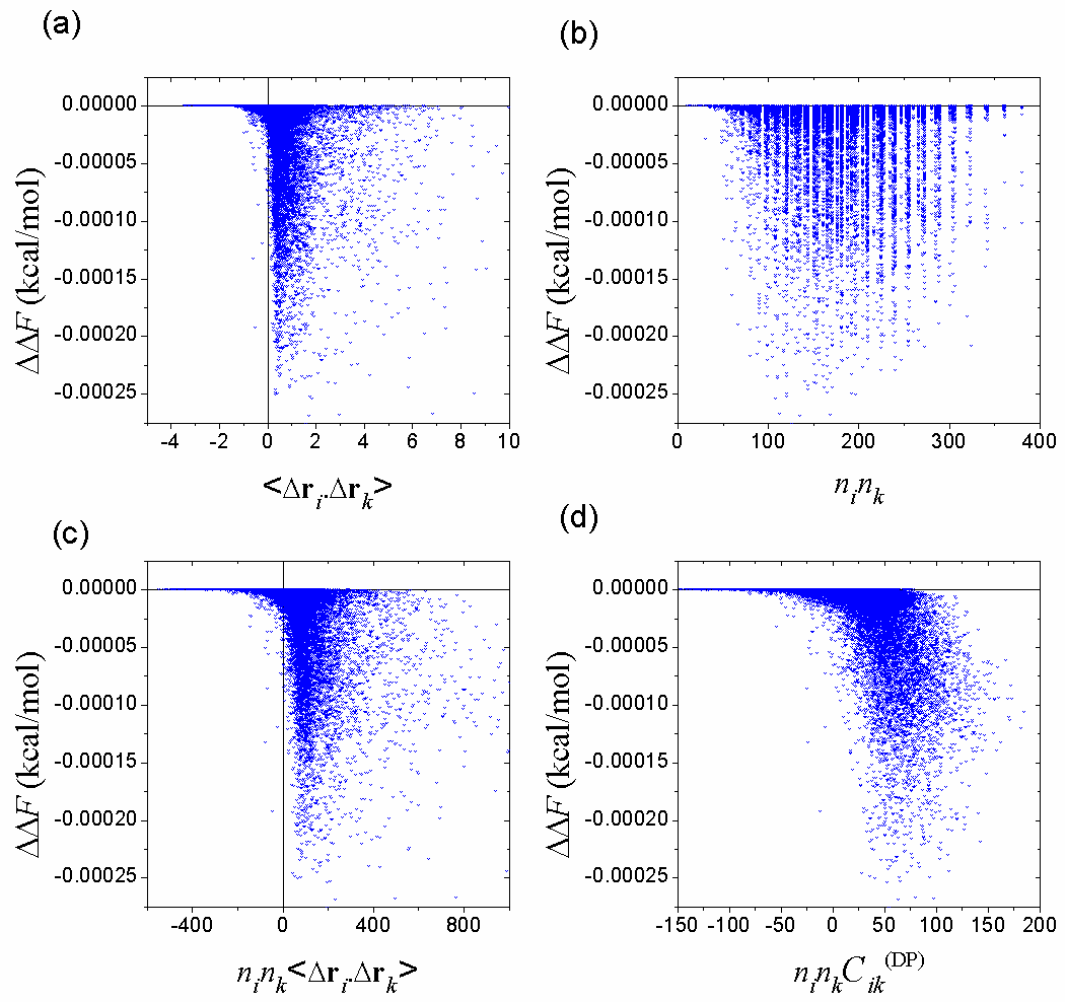

FIGURE S4 Calculated coupling free energy $\Delta\Delta F$ of dynamics-driven allostery in CAP with respect to (a) the scalar cross-correlation $\langle \Delta\mathbf{r}_i \cdot \Delta\mathbf{r}_k \rangle$ (in Å^2), (b) the product of the number of springs connected to the mutated residues ($n_i n_k$), (c) $n_i n_k \langle \Delta\mathbf{r}_i \cdot \Delta\mathbf{r}_k \rangle$ and (d) $n_i n_k C_{ik}^{(\mathrm{DP})}$. $r_\mathrm{c} = 9$Å, $m = 0.11$ kg/mol, $\gamma = 1.0$ kcal/(mol·Å^2), and $\Delta\gamma = 0.1$ kcal/(mol·Å^2) were used in the calculations.

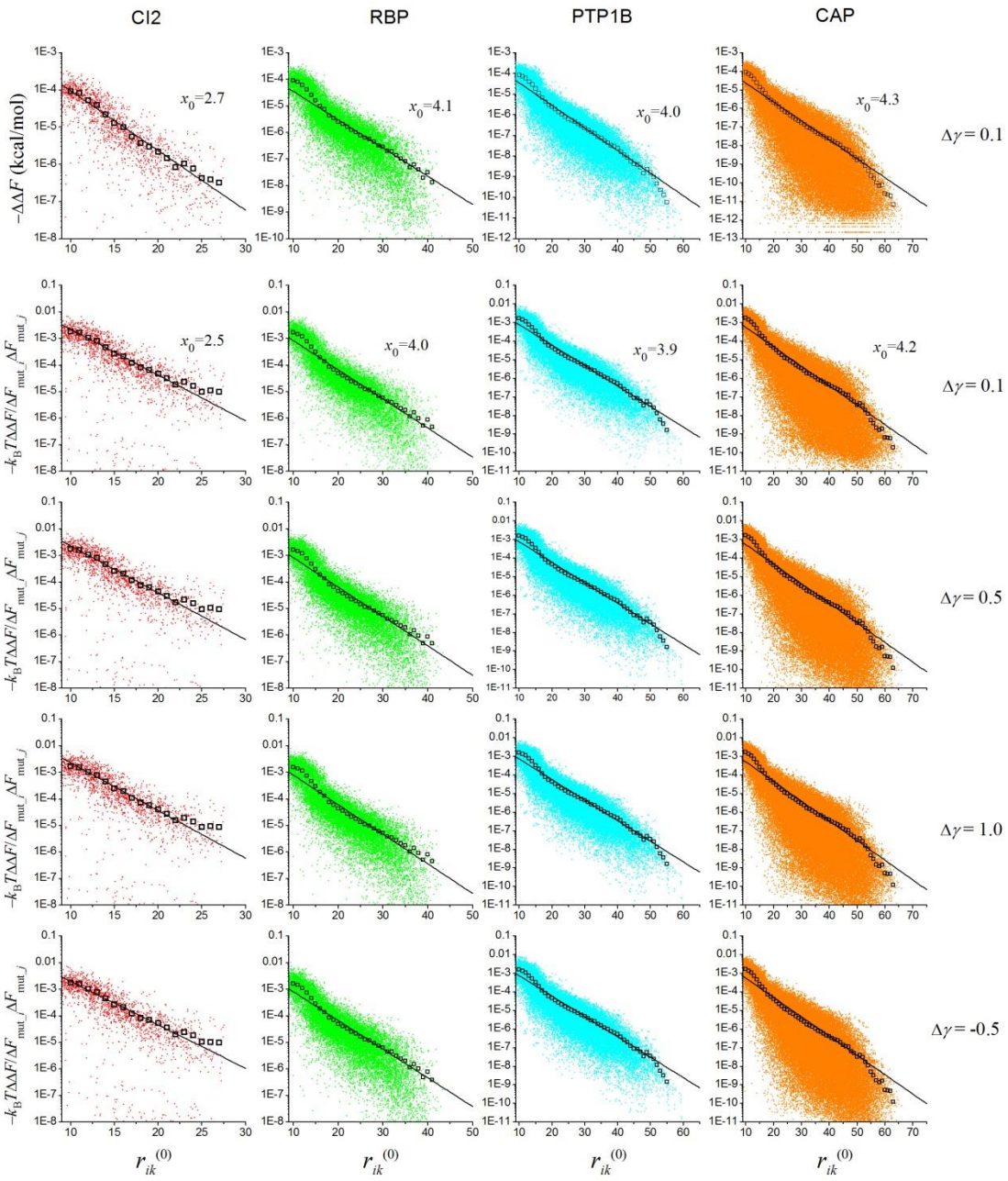

FIGURE S5 Allostery free energy ($\Delta\Delta F$) and coefficient ($\frac{k_B T\Delta\Delta F}{\Delta F_{\mathrm{mut\_}i}\Delta F_{\mathrm{mut\_}k}}$) plotted against $r_{ik}^{(0)}$ for the four protein systems (from left to right) under different $\Delta\gamma$ values (from top to bottom). The average values as a function of r_{ik} are plotted as black squares with the exponential fits ($y \propto e^{-x/x_0}$) given as solid lines. The fitted x_0 (in Å) are listed in the top two rows. $r_c = 9$ Å, $m = 0.11$ kg/mol, and $\gamma = 1.0$ kcal/(mol·Å²) were used in the calculations.

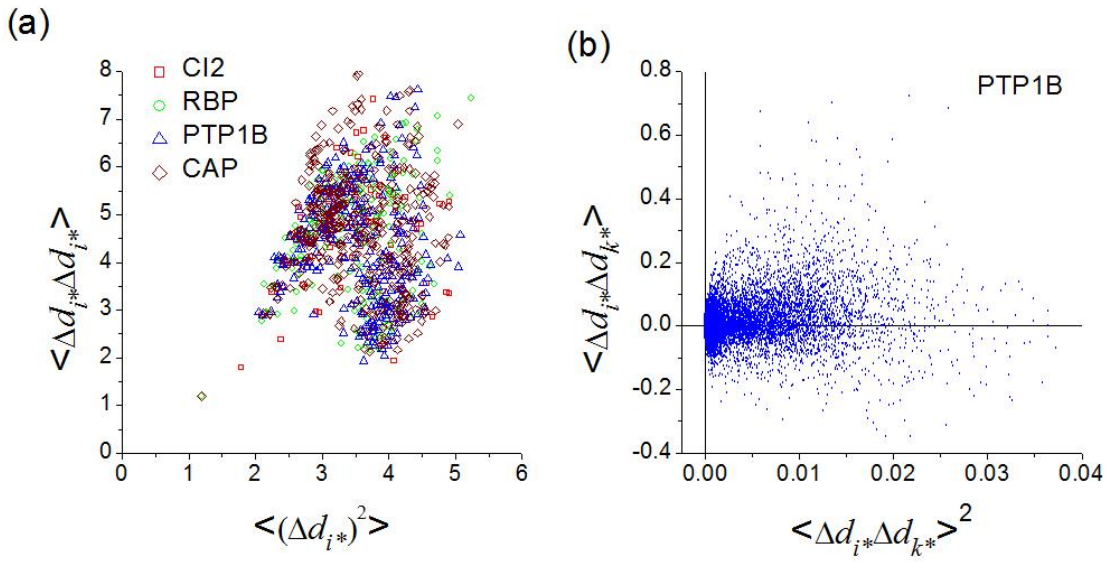

FIGURE S6 Poor correlation between dynamics-driven and structure-driven allostery coefficients. (a) Correlation between $\langle \Delta d_{i*} \Delta d_{i*} \rangle$ [Eq. (43)] and $\langle (\Delta d_{i*})^2 \rangle$ [Eq. (40)] for the four systems, which describe single residue mutation effects. (b) Correlation between $\langle \Delta d_{i*} \Delta d_{k*} \rangle$ [Eq. (44)] and $\langle \Delta d_{i*} \Delta d_{k*} \rangle^2$ [Eq. (41)], which describe the allosteric effects under a double residue mutation.

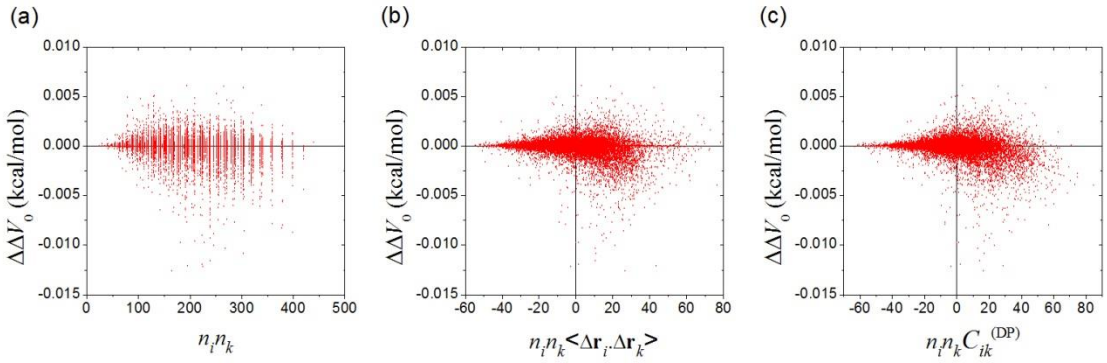

FIGURE S7 Calculated coupling equilibrium potential ($\Delta\Delta V_0$) of structure-driven allostery in PTP1B plotted against to (a) the product of the number of springs connected to the mutated residues ($n_i n_k$), (b) $n_i n_k \langle \Delta \mathbf{r}_i \cdot \Delta \mathbf{r}_k \rangle$ and (c) $n_i n_k C_{ik}^{(\mathrm{DP})}$. $r_c = 9$ Å, $m = 0.11$ kg/mol, $\gamma = 1.0$ kcal/(mol·Å^2), and $\Delta a = 0.1$ Å were used in the calculations.

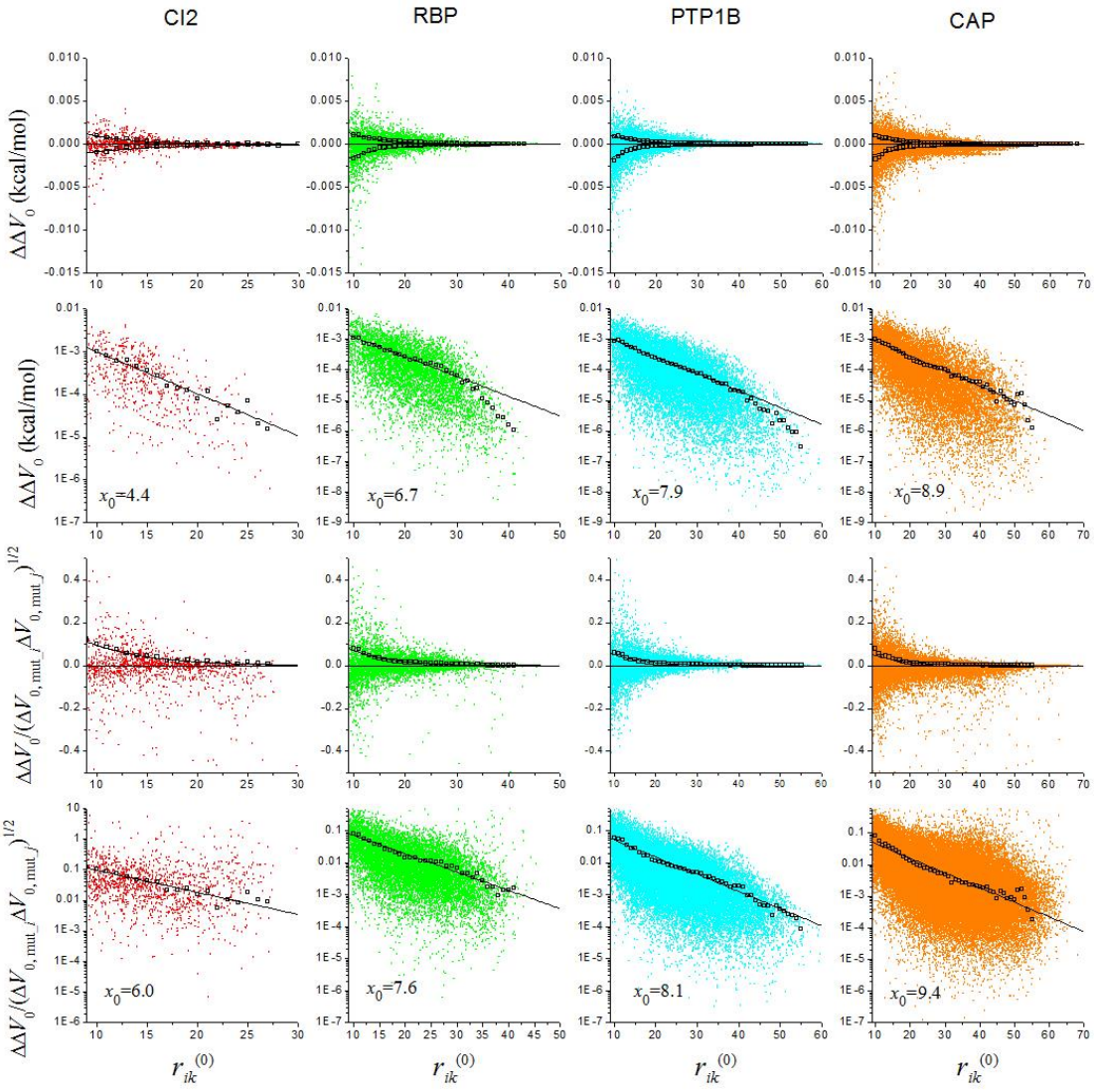

FIGURE S8 $\Delta\Delta V_0$ and $\frac{\Delta\Delta V_0}{(\Delta V_{0,\mathrm{mut\_}i}\Delta V_{0,\mathrm{mut\_}j})^{1/2}}$ with respect to $r_{ik}^{(0)}$ for the four proteins in both linear and logarithmic scales. The average values as a function of $r_{ik}^{(0)}$ are plotted as black squares with the exponential fits ($y \propto e^{-x/x_0}$) presented as solid lines. The fitted x_0 (in Å) are listed in some panels. $r_c = 9$ Å, $m = 0.11$ kg/mol, $\gamma = 1.0$ kcal/(mol·Å²) and $\Delta a = 0.1$ Å were used in the calculations.

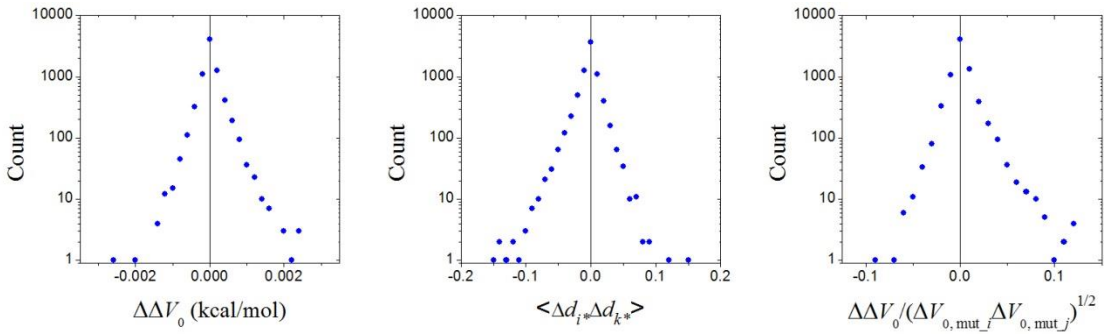

FIGURE S9 Distribution of $\Delta\Delta V_0$, $\langle \Delta d_{i*} \Delta d_{k*} \rangle$ and $-\frac{k_B T \Delta\Delta F}{\Delta F_{\mathrm{mut\_}i} \Delta F_{\mathrm{mut\_}k}}$ data with $20\text{Å} \leq r_{ik} \leq 25\text{Å}$ for PTP1B. $r_c = 9$ Å, $m = 0.11$ kg/mol, $\gamma = 1.0$ kcal/(mol·Å²) and $\Delta a = 0.1$ Å were used in the ANM calculations.